Cell Research (2011) 21:305-315.

www.nature.com/cr

ORIGINAL ARTICLE

Graded activation of CRAC channel by binding of different numbers of STIM1 to Orai1 subunits

Zhengzheng Li[1, *], Lin Liu[2, *], Yongqiang Deng[1, *], Wei Ji[1], Wen Du[1], Pingyong Xu[1], Liangyi Chen[1], Tao Xu[1, 2]

[1]*National Key Laboratory of Biomacromolecules, Institute of Biophysics, Chinese Academy of Sciences, Beijing 100101, China;*
[2]*College of Life Science and Technology, Huazhong University of Science and Technology, Wuhan 430074, China*

The Ca^{2+} release-activated Ca^{2+} (CRAC) channel pore is formed by Orai1 and gated by STIM1 after intracellular Ca^{2+} store depletion. To resolve how many STIM1 molecules are required to open a CRAC channel, we fused different numbers of Orai1 subunits with functional two-tandem cytoplasmic domains of STIM1 (residues 336-485, designated as S domain). Whole-cell patch clamp recordings of these chimeric molecules revealed that CRAC current reached maximum at a stoichiometry of four Orai1 and eight S domains. Further experiments indicate that two-tandem S domains specifically interact with the C-terminus of one Orai1 subunit, and CRAC current can be gradually increased as more Orai1 subunits can interact with S domains or STIM1 proteins. Our data suggest that maximal opening of one CRAC channel requires eight STIM1 molecules, and support a model that the CRAC channel activation is not in an "all-or-none" fashion but undergoes a graded process via binding of different numbers of STIM1.

***Keywords*:** CRAC channel; Orai1; STIM1; calcium store; stoichiometry
Cell Research (2011) **21**: 305-315. doi:10.1038/cr.2010.131; published online 14 September 2010

Introduction

Activation of cell surface receptors that activate phospholipase C causes Ca^{2+} release from the endoplasmic reticulum (ER) Ca^{2+} store. The resulting depletion of intracellular Ca^{2+} store induces extracellular Ca^{2+} influx through CRAC channels [1, 2]. STIM1 [3, 4] and Orai1 [5-7] are essential proteins of the CRAC channel. STIM1 is localized at the ER and functions as the sensor of ER luminal Ca^{2+} concentration [3, 8], and Orai1 is the channel pore subunit at the plasma membrane (PM) [9-11]. STIM1 aggregates underneath the PM after store depletion [3, 12-14] and activates the CRAC channel by directly binding to Orai1 [15, 16].

Knowledge of the stoichiometry of the CRAC channel is crucial to understanding the mechanisms of channel assembly, gating and function. We and others have previously demonstrated that Orai1 forms tetramers in the PM [17-20]. We have also demonstrated that one CRAC channel contains at least two STIM1 full-length cytosolic fragments (CT-STIM1) [17-20], which suggests that a STIM1 dimer may be enough to open the CRAC channel. This result seems to disagree with the general belief that the oligomerization of full-length STIM1 is required for the channel activation [21, 22]. It should be pointed out that in the previous paper [17], we deliberately expressed STIM1 at very low levels to ensure the detection of single molecule fluorescence, and did not document whether there was full activation of Orai1 channels at those low levels of CT-STIM1 expression. Thus, it remains unclear whether the Orai1 activated by CT-STIM1 and the Orai1 activated by full-length STIM1 after store depletion are of the same stoichiometry. Therefore, how many STIM1 molecules are required to fully activate a CRAC channel remains an open question. Recently, small cytosolic fragments of STIM1, such as SOAR (residues 344-442) [23] and CAD (residues 342-448) [15] have been identified as core domains of STIM1 that efficiently activate Orai1 channels without depletion of ER Ca^{2+} stores. These functional fragments provide us a substitution of the full-length STIM1 in activating CRAC channel. Inspired by the approach that utilized fusing chimeras of the L-type Ca^{2+} channel and calmodulin to

*These three authors contributed equally to this work.
Correspondence: Tao Xu[a], Liangyi Chen[b]
[a]E-mail: xutao@ibp.ac.cn
[b]E-mail: chen_liangyi@yahoo.com
Received 21 July 2010; revised 9 August 2010; accepted 11 August 2010; published online 14 September 2010

investigate the stoichiometry of channel/calmodulin interaction in Ca^{2+}-dependent channel inactivation [24], we linked Orai1 with different numbers of functional STIM1 domain to investigate the STIM1/Orai1 stoichiometry in the activation of the CRAC channel.

Results

Orai1 linked with cytosolic STIM1 fragments produces constitutive CRAC-like current

We chose functional cytosolic STIM1 fragments with less tendency to aggregate to avoid excessive interactions between STIM1 fragments that might affect the assembly and transport of the linked Orai1 subunits. An initial attempt using SOAR domain was not successful, because the SOAR-linked Orai1 tended to form aggregates in the ER without being transported to the PM. Most functional cytosolic STIM1 fragments purified *in vitro* form dimmers [16, 23], and CAD forms tetramers [15]. Hence, we next selected the dimeric STIM1 fragment (residues 336-485), termed as S domain here, which activates the Orai1 channel efficiently [23]. First, tandem S domains (SS) were constructed by linking two S domains with a 24-amino acid linker sequence (L1 in Figure 1A; see Methods and Supplementary information, Figure S1 for constructs used in this study). Coexpressing Orai1 with dimeric SS domains generated constitutive CRAC-like currents in HEK293 cells, whereas no observable current

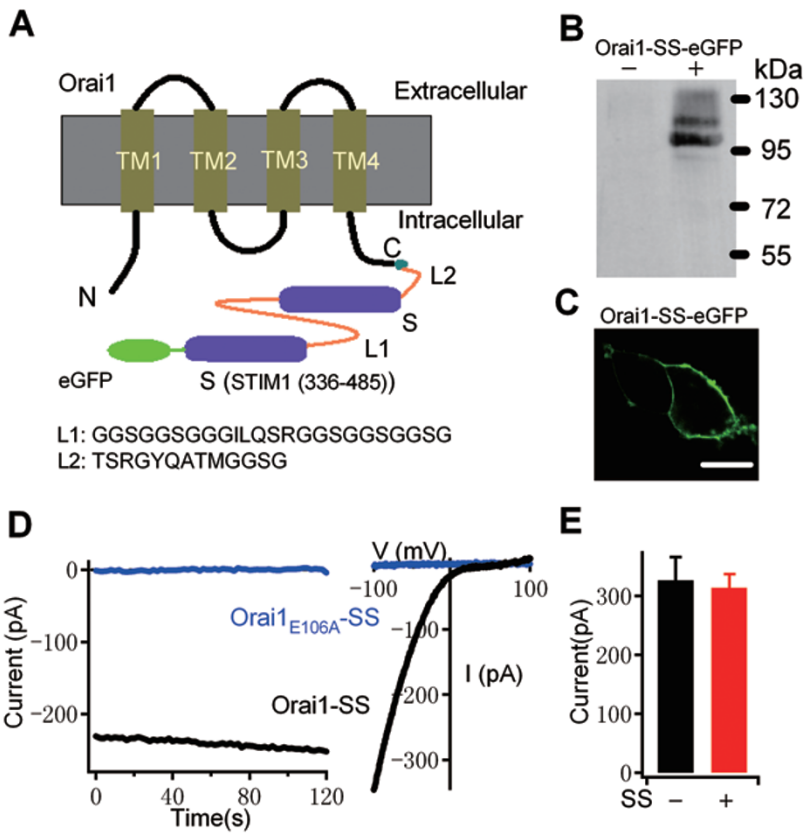

Figure 1 Orai1-SS generated constitutive, fully activated I_{CRAC}. **(A)** Schematic diagram of Orai1-SS-eGFP. S, Stim1 (336-485). Tandem S domains (SS) were created by covalently fusing two S domains with a 24-amino acid linker sequence (L1). The Orai1 subunit is attached intracellularly to SS using a 13-amino acid linker sequence (L2). The sequences of L1 and L2 are indicated at the bottom. **(B)** Western blots of non-tranfected cells and cells transfected with Orai1-SS-eGFP, visualized with GFP-specific antibody. **(C)** Location at the PM of Orai1-SS-eGFP in HEK293 cells. Images were captured at the middle plane using confocal microscopy. Scale bar, 10 μm. **(D)** Left: representative time courses of I_{CRAC} evaluated at −80 mV in HEK293 cells transfected with Orai1-SS-eGFP (black) or $Orai1_{E106A}$-SS-eGFP (blue). Cells were bathed in external solution containing 6 mM Ca^{2+} and dialyzed with internal solution with free Ca^{2+} buffered to 145 nM by $CaCl_2$ and BAPTA. Currents were plotted after break-in. Right: characteristic leak-subtracted I-V relationships for I_{CRAC} recorded in the same cells from the left panel. Data were representative of more than five cells. **(E)** Additional SS did not contribute to I_{CRAC} of Orai1-SS. Summary (mean ± s.e.m.) of I_{CRAC} amplitudes at −100 mV in cells expressing Orai1-SS-eGFP alone (black; n = 13) or together with SS-mKO (red; n = 12).

was recorded in cells expressing SS alone (Supplementary information, Figure S2), consistent with the low level of endogenous Orai1 in HEK293 cells. Then, we fused a single Orai1 subunit to the N-terminus of SS to generate an eGFP-tagged Orai1-SS (Orai1-SS-eGFP) with a stoichiometry of one Orai1 subunit and two S domains (Figure 1A). Western blotting of HEK293 cells transfected with Orai1-SS-eGFP detected bands at ~100 kDa, consistent with the predicted molecular mass of Orai1-SS-eGFP and confirming that the intact full-length chimeric protein was properly expressed (Figure 1B). Orai1-SS-eGFP was properly translocated to the PM as confirmed by confocal fluorescence imaging (Figure 1C). Using whole-cell patch clamp recording, large spontaneous currents with inwardly rectifying I-V curves were recorded in HEK293 cells expressing Orai1-SS-eGFP (Figure 1D). These currents shared many characteristics of native I_{CRAC} current, such as an inwardly rectifying I/V relationship, dependence on extracellular Ca^{2+}, permeability to Na^{+} in divalent-free solution (DVF), sequential potentiation and inhibition by 100 μM 2-APB and blockade by La^{3+} (Supplementary information, Figure S3). No current was observed when wild-type (WT) Orai1 was substituted with a non-conducting $Orai1_{E106A}$ mutant [9] (Figure 1D), confirming that the current was mediated by the Orai1 subunit in Orai1-SS. Thus, this self-activated current indicates that the SS domain fused to Orai1 was not only correctly targeted, but also fully functional.

CRAC channel formed by Orai1-SS reaches the maximal activation level

To test whether the CRAC channel formed by Orai1-SS was maximally activated, currents in cells expressing Orai1-SS-eGFP either alone or together with SS-monomeric Kushibara Orange (mKO) were compared. To control expression levels of Orai1 proteins, we selected cells with similar total GFP fluorescence (Supplementary information, Figure S4) for recording. We verified that the cell surface portion of Orai1-containing chimeras was not altered by coexpression of SS domains (Supplementary information, Figure S4H). This fluorescence-based control of channel protein levels was employed throughout the study whenever comparison between different constructs was made (see Materials and Methods). We reasoned that if Orai1-SS did not provide enough S domains to fully activate the CRAC channel, supplying additional S domains to the channel pore should augment the currents. However, the I_{CRAC} produced by coexpression of Orai1-SS-eGFP with SS-mKO showed a similar amplitude (314 ± 23 pA, n = 12) compared to that of Orai1-SS-eGFP expressed alone (327 ± 40 pA, n = 13; Figure 1E), suggesting that CRAC channels formed by Orai1-SS reach the maximum. Coexpression of SS-eGFP did not enhance the I_{CRAC} produced by Orai1-SS fused with a smaller 3× Flag tag either (Supplementary information, Figure S5A). Increasing the linker length between the Orai1 and the SS domain to 44 amino acids (Orai1-L_{44}-SS) generated similar currents in amplitude compared with the original Orai1-SS (Supplementary information, Figure S5B), indicating that neither the tag nor the linker perturb the channel activation. The attempt to link Orai1 with three tandem S domains was not successful as Orai1-SSS exhibited enhanced accumulation in intracellular compartments and reduced I_{CRAC} amplitudes (Supplementary information, Figure S5C and S5D).

It is not known whether an Orai1-SS tetramer is cross-activated by S domains from a nearby channel rather than its own SS domains. To address this uncertainty, we coexpressed the non-conducting $Orai1_{E106A}$-SS-eGFP with mKO-tagged four-tandem Orai1 (4×Orai1-mKO). Both constructs were trafficked to the PM. As the four-tandem Orai1 (4×Orai1) itself assembles to form a CRAC channel without interacting with other Orai1 subunits [17, 18], 4×Orai1 would be activated by S domains from $Orai1_{E106A}$-SS, if cross-interaction is possible. However, no I_{CRAC} was recorded in cells coexpressing 4×Orai1-mKO and $Orai1_{E106A}$-SS-eGFP, as compared to large spontaneous I_{CRAC} reconstituted by coexpression of 4×Orai1-mKO with SS-eGFP (Figure 2A). Therefore, these results exclude the possibility of a cross-activation of the Orai1 channel by S domains from neighboring Orai1-SS protein, and indicate that Orai1-SS functions through self-interaction inside an assembled channel.

Both S domains of Orai1-SS contribute to the activation of Orai1 channel

The linkers in Orai1-SS (L1 and L2 in Figure 1A) might constrain the free movement of the S domains and hinder the interaction of either S domain with the Orai1 protein. To address this issue, we introduced the LQ347/348AA mutation in either S domain within Orai1-SS-eGFP. The LQ347/348AA mutation has been shown to abolish the ability of STIM1 and SOAR to activate Orai1 [23]. Consistent with that report, overexpressing $S_{LQ/AA}$ with Orai1 in HEK293 cells generated much reduced CRAC current as compared with cells transfected with WT S domain and Orai1, despite the association of $S_{LQ/AA}$ with Orai1 at the PM (Supplementary information, Figure S6). Similarly, Orai1-$S_{LQ/AA}$S and Orai1-$SS_{LQ/AA}$ generated equally reduced constitutive I_{CRAC} compared with Orai1-SS (Orai1-SS, 364 ± 24 pA, n = 10; Orai1-$S_{LQ/AA}$S, 176 ± 14 pA, n = 12; Orai1-$SS_{LQ/AA}$, 174 ± 16 pA, n = 12; Figure 2B). This suggests that there is no selectivity or priority in either S domain of Orai1-SS for

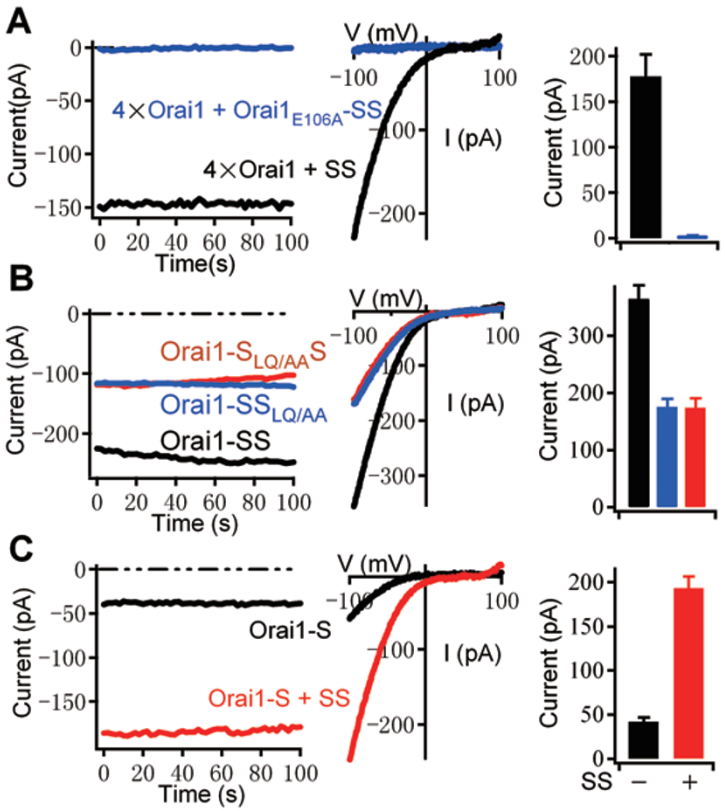

Figure 2 The CRAC channel formed by Orai1-SS is activated by the covalently associated S domains and both S domains of Orai1-SS participate in activating the channel. **(A)** S domains in Orai1$_{E106A}$-SS could not activate channels formed by 4×Orai1. Left: time courses of I_{CRAC} in cells expressing 4×Orai1-mKO together with either SS-eGFP (black) or Orai1$_{E106A}$-SS-eGFP (blue). Middle: representative I-V relationships form the same cells as in the left. Right: average current amplitudes at −100 mV of nine cells in each condition. **(B)** LQ/AA mutation in either S domain of Orai1-SS reduced the current amplitude equally. Representative time courses (left), I-V relationships (middle) and summary of current amplitudes (right) of cells transfected with Orai1-SS-eGFP (black; *n* = 10), Orai1-SS$_{LQ/AA}$-eGFP (blue; *n* = 12) or Orai1-S$_{LQ/AA}$S-eGFP (red; *n* = 12). **(C)** The I_{CRAC} generated by Orai1-S was augmented by additional S domains. Representative time courses (left), I-Vs (middle) and average current amplitudes (right) of cells expressing Orai1-S-eGFP alone (black; *n* = 10) or together with SS-mKO (red; *n* = 13). Averaged data are presented as mean ± s.e.m.

channel activation. Moreover, eGFP-tagged construct composed of one Orai1 subunit fused to one S domain (Orai1-S-eGFP) generated reduced constitutive I_{CRAC} (42 ± 5 pA, *n* = 10) and this current was augmented by coexpression of SS-mKO (193 ± 14 pA, *n* = 13; Figure 2C), suggesting that the single S domain in Orai1-S does not maximally open the associated Orai1 channel. These results indicate that both S domains of Orai1-SS participate in the activation of the linked Orai1 channel.

I_{CRAC} amplitude depends on the number of S domains linked to Orai1 subunits

The reduced I_{CRAC} generated by Orai1-S as compared with Orai1-SS suggests that CRAC channel may not be maximally opened when presented with fewer than eight S domains. To test this possibility, we fused SS to the two-tandem Orai1 (2×Orai1-SS) and to the four-tandem Orai1 (4×Orai1-SS). As two-tandem Orai1 dimerizes to form a CRAC channel pore and four-tandem Orai1 forms a channel pore by itself [17], 2×Orai1-SS and 4×Orai1-SS would generate channels associated with four S and two S domains, respectively. Expression of full-length 2×Orai1-SS-eGFP and 4×Orai1-SS-eGFP vectors was confirmed by western blotting (Figure 3A) and their location at the PM was determined by confocal imaging (Figure 3B). Similar to Orai1-S, cells expressing 2×Orai1-SS-eGFP (Figure 3C) generated a small I_{CRAC} (45 ± 3 pA, *n* = 12). Coexpression of SS-mKO with 2×Orai1-SS-eGFP augmented the current amplitude ~4-fold (195 ± 23 pA, *n* = 12; Figure 3C). Similar current amplitudes were

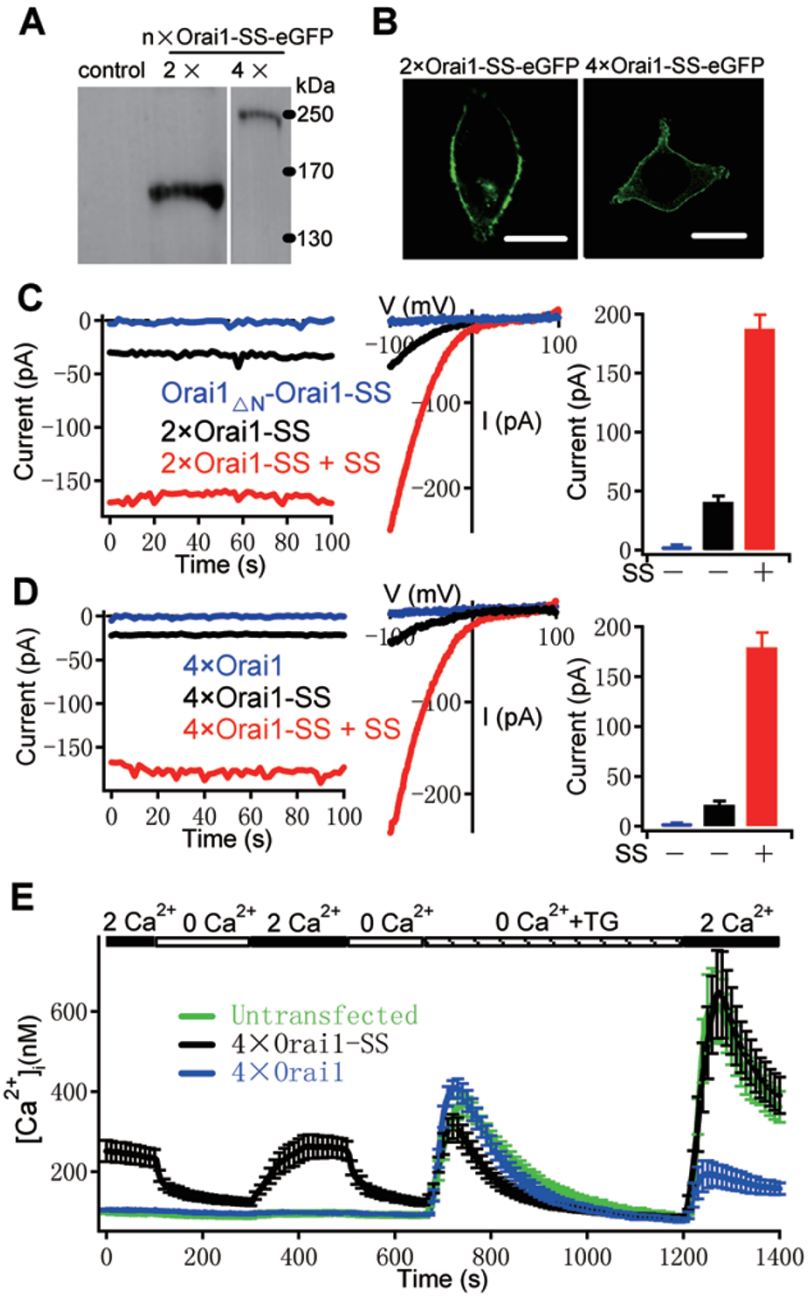

Figure 3 Partial activation of the CRAC channel by four and two S domains. **(A)** Western blots of cells transfected with 2×Orai1-SS-eGFP or 4×Orai1-SS-eGFP, using GFP-specific antibody. Untransfected cells were used as control. **(B)** 2×Orai1-SS-eGFP and 4×Orai1-SS-eGFP were dominantly located at the PM under confocal microscopy. Scale bars, 10 μm. **(C)** 2×Orai1-SS generated constitutive current and the current was augmented by additional SS. Left: representative time courses of I_{CRAC} in cells expressing $Orai1_{\Delta N}$-Orai1-SS-eGFP (blue), 2×Orai1-SS-eGFP (black) or 2×Orai1-SS-eGFP together with SS-mKO (red). Middle: characteristic I-Vs from the same cells in the left panel. Right: average current amplitudes (mean ± s.e.m.) of cells transfected with $Orai1_{\Delta N}$-Orai1-SS-eGFP (n = 7), 2×Orai1-SS-eGFP (n = 9) or 2×Orai1-SS-eGFP together with SS-mKO (n = 10). **(D)** Time courses (left), I-Vs (middle) and averages (right; mean ± s.e.m.) of I_{CRAC} in cells expressing 4×Orai1-eGFP (blue; n = 11), 4×Orai1-SS-eGFP (black; n = 11) or 4×Orai1-SS-eGFP together with SS-mKO (red; n = 13). **(E)** 4×Orai1-SS activated Ca^{2+} influx without depleting intracellular Ca^{2+} stores. Mean ± s.e.m. of Ca^{2+} measurements in untransfected HEK293 cells (green; n = 15) and cells expressing 4×Orai1-eGFP (blue; n = 15), 4×Orai1-SS-eGFP (black; n = 19) are shown. Solution exchange is indicated by the bars. 1 μM TG in Ca^{2+}-free solution was used to deplete Ca^{2+} stores.

observed when the linker between the two-tandem Orai1 and SS was lengthened to 44 amino acids (Supplementary information, Figure S7A and S7B). It remains possible that four 2×Orai1-SS interact with each other and each contributes one Orai1 subunit to form a channel pore with eight interacting S domains. Therefore, we generated a construct with the N-terminus (residues 1-90) of the first Orai1 subunit truncated ($Orai1_{\Delta N}$-Orai1-SS-eGFP), which was unable to conduct current as shown previously. Arguing against that possibility, overexpressing $Orai1_{\Delta N}$-Orai1-SS in HEK293 cells failed to reconstitute any currents (Figure 3C), although it was efficiently trafficked to the PM (Supplementary information, Figure S7G). These results suggest that four S domains do open the CRAC channel and more S domains are required to maximize I_{CRAC}. Similarly, patch clamp experiments revealed small spontaneous I_{CRAC} in cells expressing 4×Orai1-SS-eGFP (Figure 3D) or 4×Orai1-L_{44}-SS (Supplementary information, Figure S7D and S7E). The current generated by 4×Orai1-SS-eGFP was enhanced by about 9-fold (179 ± 15 pA, n = 13) by coexpression of SS-mKO (Figure 3D). No I_{CRAC} was observed in cells expressing 4×Orai1-eGFP alone (Figure 3D), indicating that the small current did not result from spontaneous activation of the concatenated Orai1 tetramer by endogenous STIM1. We also measured free cytoplasmic Ca^{2+} concentration ($[Ca^{2+}]_i$) to further examine the store-operated Ca^{2+} entry (SOCE) in cells expressing these vectors. Compared with untransfected cells and cells transfected with 4×Orai1-eGFP, cells expressing 4×Orai1-SS-eGFP showed higher basal $[Ca^{2+}]_i$ and spontaneous Ca^{2+} influx without depleting intracellular stores (Figure 3E), in full agreement with the electrophysiological recordings and our previous finding [17]. In addition, after thapsigargin (TG)-induced depletion of Ca^{2+} from the ER, cells transfected with 4×Orai1-SS-eGFP showed slightly larger Ca^{2+} influx. In contrast, SOCE in cells transfected with 4×Orai1-eGFP was largely suppressed (Figure 3E), similar to previous reports that overexpression of WT Orai1 inhibited endogenous I_{CRAC} [14, 25, 26].

Graded activation of CRAC channel by activating different numbers of Orai1 subunits

To test directly whether the multiple levels of CRAC current resulted from different numbers of Orai1 subunit being activated, we sought to find a mutant that selectively perturb the activation of individual subunit in the channel complex. The mutation of Orai1 at position 273 (L273S) has been reported to prevent the interaction of the cytosolic C-terminus of Orai1 with STIM1 and hence the activation by STIM1 [27]. Similarly, coexpression of SS or STIM1 with $Orai1_{L273S}$ failed to generate I_{CRAC} current in our hands (Supplementary information, Figure S8A and S8B). To our surprise, $Orai1_{L273S}$-SS exhibited large constitutive I_{CRAC} (Supplementary information, Figure S8C), while the I_{CRAC} amplitudes decreased when the linker between $Orai1_{L273S}$ and SS is lengthened to 44 amino acids (Supplementary information, Figure S8D). These results imply that the short linker might force the SS domain to interact with $Orai1_{L273S}$ despite a reduced affinity. We speculated that a mutation of L273 to a polar, charged amino acid would be stronger than the L273S mutation and might abolish the activation of Orai1 by the linked S domains. Indeed, unlike $Orai1_{L273S}$-SS, tethered SS domains ($Orai1_{L273D}$-SS) were not able to activate $Orai1_{L273D}$, though $Orai1_{L273D}$-SS was efficiently trafficked to the PM (Figure 4A and 4C). In addition, soluble SS could not be recruited to the PM by $Orai1_{L273D}$, and expression of $Orai1_{L273D}$ together with either SS or STIM1 did not generate observable I_{CRAC} (Figure 4B, 4D and 4E). These results suggest that the L273D replacement in Orai1, like its forerunner L273S, disrupts the proper interaction between Orai1 and STIM1, and thus abolishes the channel activation.

Therefore, we introduced the L273D mutation in the 4×Orai1-SS-eGFP to generate a series of constructs containing one ($Orai1_{L273D}$-3×Orai1-SS), two (2×$Orai1_{L273D}$-2×Orai1-SS), three (3×$Orai1_{L273D}$-Orai1-SS) and four mutated (mut) subunits (4×$Orai1_{L273D}$-SS). Channels composed of different combination of mut and WT Orai1 subunits could thus be produced. Patch clamp recording of cells expressing each of these constructs alone or together with SS-mKO showed the following (Figure 5A): (1) Overexpression of 4×$Orai1_{L273D}$-SS alone or with SS in HEK293 cells failed to reconstitute I_{CRAC}, consistent with the inability of $Orai1_{L273D}$ to interact with SS domains. (2) Expression of 3×$Orai1_{L273D}$-Orai1-SS, 2×$Orai1_{L273D}$-2×Orai1-SS and $Orai1_{L273D}$-3×Orai1-SS alone generated currents with similar amplitudes to those generated by expression of 4×Orai1-SS, indicating that the current was generated by a single Orai1 bound with SS in the CRAC channel. (3) Coexpression of SS did not augment the I_{CRAC} of 3×$Orai1_{L273D}$-Orai1-SS but led to graded increase in the I_{CRAC} of 2×$Orai1_{L273D}$-2×Orai1-SS, $Orai1_{L273D}$-3×Orai1-SS and 4×Orai1-SS.

To examine whether full-length STIM1 also opened the CRAC channel upon Ca^{2+} store depletion in a graded fashion, we utilized a series of four-tandem heterozygous mut/WT Orai1 constructs that contained one ($Orai1_{L273D}$-3×Orai1), two (2×$Orai1_{L273D}$-2×Orai1), three (3×$Orai1_{L273D}$-Orai1) and four $Orai1_{L273D}$ subunits (4×$Orai1_{L273D}$). Each of these constructs or 4×Orai1-eGFP was coexpressed with mOrange-tagged STIM1 (STIM1-mOrange) in HEK293 cells. Except for the 4×$Orai1_{L273D,}$

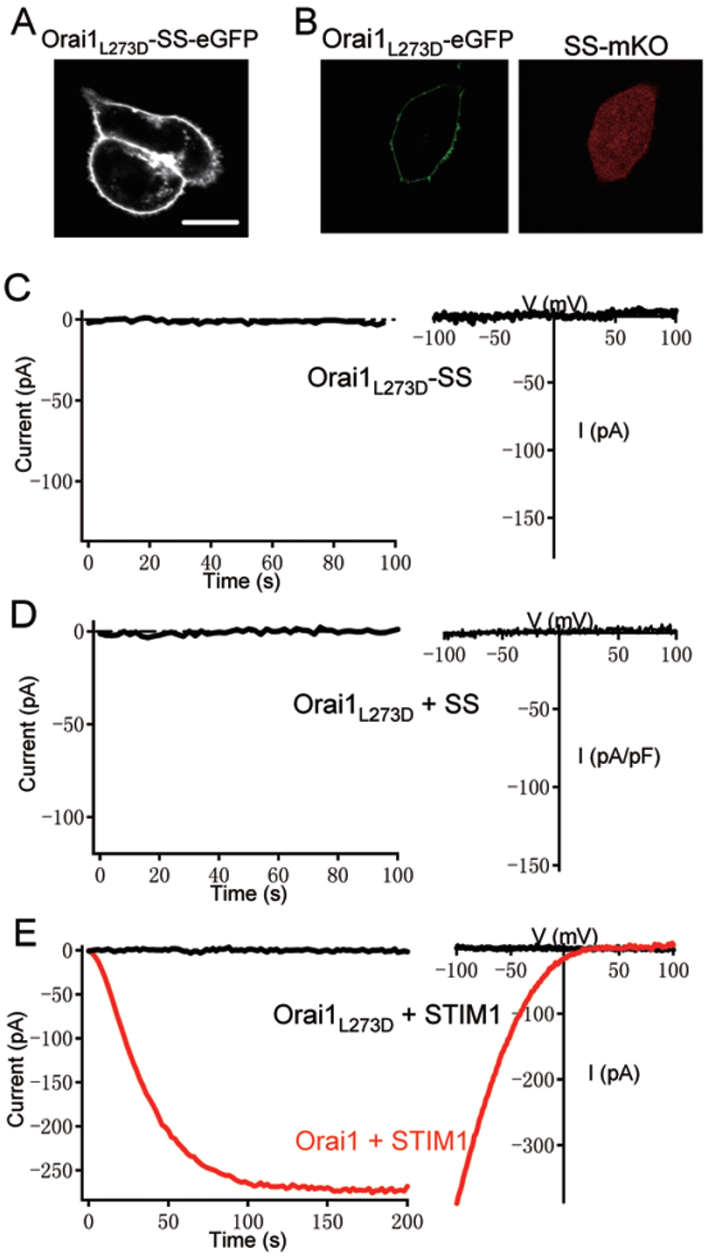

Figure 4 L273D mutation of Orai1 abolishes the I_{CRAC} of Orai1-SS. **(A)** $Orai1_{L273D}$-SS-eGFP was efficiently translocated to the plasma membrane as shown by confocal imaging. **(B)** $Orai1_{L273D}$-eGFP was efficiently translocated to the PM (left) but could not recruit coexpressed SS-mKO (right). Images were captured at the middle plane using confocal microscopy. **(C)** $Orai1_{L273D}$-SS did not produce self-activated I_{CRAC}. Representative time courses (left) and I-V relationships (right) of cells transfected with $Orai1_{L273D}$-SS-eGFP. **(D)** No I_{CRAC} was observable in cells cotransfected with SS-mKO and $Orai1_{L273D}$-eGFP. **(E)** $Orai1_{L273D}$ could not be activated by STIM1 after store depletion. Cells were cotransfected with STIM1-mOrange + Orai1-eGFP (red) or STIM1-mOrange + $Orai1_{L273D}$-eGFP (black). Data are representatives of more than three cells in each condition.

all the other constructs reconstituted I_{CRAC} in patch clamp experiments with a pipette solution containing 10 μM inositol 1,4,5-trisphosphate ($Ins(1,4,5)P_3$) to deplete Ca^{2+} stores (Figure 5B and 5C). The I_{CRAC} amplitudes increased as the number of WT subunits in the vector increased (Figure 5D): 21 ± 4.0 pA for 3×$Orai1_{L273D}$-Orai1, 61 ± 12 pA for 2×$Orai1_{L273D}$-2×Orai1, 157 ± 25 pA for $Orai1_{L273D}$-3×Orai1 and 290 ± 43 pA for 4×Orai1. Thus, graded augmentation of CRAC channel is not limited to SS domains, but also occurs with full-length STIM1 un-

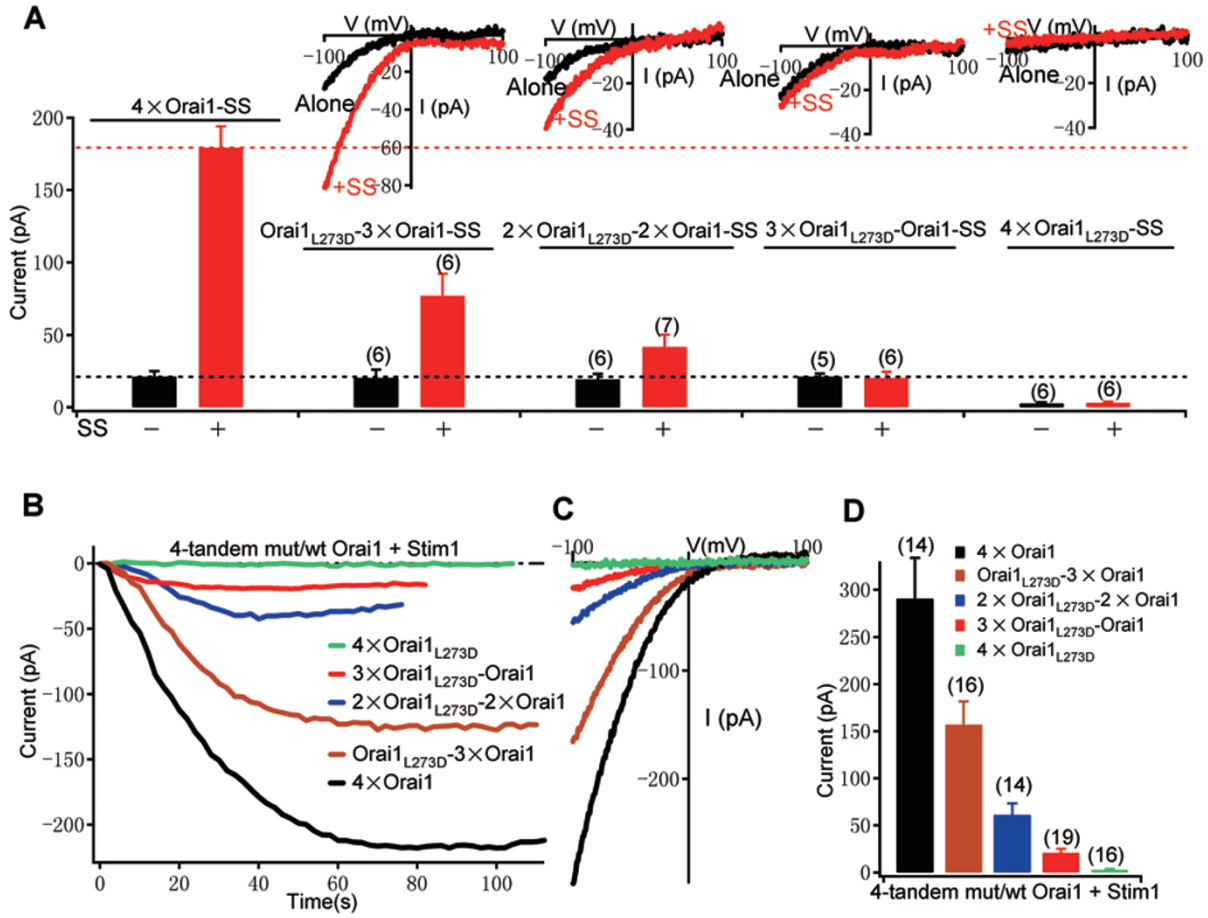

Figure 5 Two S domains open the Orai1 channel through specifically interacting with one Orai1 subunit, and coexpressed S domains or STIM1 increases I_{CRAC} gradually with the increment of WT Orai1 subunits in the channel. **(A)** Representative I-V relationships (upper) and averages (lower; mean ± s.e.m.) of cells expressing each of the four indicated eGFP-tagged constructs alone (black) or together with SS-mKO (red). Numbers of cells in each category are labeled in brackets above the columns. For comparison, I_{CRAC} averages of 4×Orai1-SS (black) or 4×Orai1-SS + SS (red) reproduced from Figure 3D. **(B)** Developments of I_{CRAC} in cells cotransfected with Stim1-mOrange and each of the eGFP-tagged four-tandem Orai1 constructs containing 0-4 $Orai1_{L273D}$ subunits. 10 μM $Ins(1,4,5)P_3$ in pipette solution was used to deplete Ca^{2+} store. **(C)** I-Vs at maximal activation for each category as marked in **(B)**. **(D)** Summary (mean ± s.e.m.) of peak current amplitudes for each category as indicated. Numbers of cells are labeled in the brackets.

der physiological stimulation.

Discussion

In the current study, we took an approach to interrogate the stoichiometry of CRAC channel by linking different numbers of Orai1 and functional S domains of STIM1 and reconstituting CRAC-like channels in HEK293 cells. Our results demonstrate that channels composed of four Orai1 and tethered eight S domains gave rise to the maximum current, which cannot be further increased by providing more soluble SS domains. Although tethering has the advantage of providing high local concentration of proteins, it may limit the effectiveness of tethered proteins by exerting geometric constraints. In our case, we believe that tethered SS domains were, at least, of the same potency in binding to and activating Orai1 channels as the soluble SS domains or full-length STIM1 for the following reasons: first, Orai1-SS generated similar currents in amplitude as Orai1 coexpressed with SS or full-length STIM1 (Supplementary information, Figure S9A). Second, coexpression of SS did not augment the current of $Orai1\text{-}SS_{LQ/AA}$ (Supplementary information, Figure S9B). Finally, channels formed by the $Orai1_{L273S}$ mutants could neither be activated by coexpressed SS (Supplementary information, Figure S8A),

nor by full-length STIM1 after store depletion (Supplementary information, Figure S8B) [27]. In contrast, tethering SS domain to $Orai1_{L273S}$ produced huge CRAC currents, which were reduced when the linker between Orai1 and SS domain was increased to 44 AA ($Orai1_{L273S}$-L_{44}-SS; Supplementary information, Figure S8C). This result suggests that tethered SS domains are indeed more efficient in activating the Orai1 channel than the soluble S domains by providing a high local concentration of S domain in the close proximity to Orai1 channel.

To further demonstrate whether all tethered eight S domains or only a portion of them contribute to the activation of tandem Orai1 chimeras, we sought to evaluate the relative contribution of each tethered SS domain. We found that the L273D mutation of Orai1 abolished the interaction between Orai1 and SS domains and hence the generation of I_{CRAC} (Figure 4). We then mixed different numbers of non-interacting $Orai1_{L273D}$ mutants and WT Orai1 subunits, and evaluated the contribution of SS binding to each Orai1 monomer in generating I_{CRAC}. Our data support that two S domains specifically interact with one Orai1 subunit and I_{CRAC} increases gradually with increment of WT Orai1 subunits upon binding of S domains. Based on above results, we propose that two STIM1 molecules can open the CRAC channel through binding to one Orai1 subunit; the opening activity of the channel increases with more Orai1 subunits bound with STIM1 and channel reaches maximal activation when all four subunits are bound with eight STIM1 molecules. This is consistent with the results that STIM1 dimerizes through its cytosolic domain at rest [21], and dimeric cytosolic domains of STIM1 can efficiently activate the Orai1 channel [28, 29]. However, we cannot, of course, completely exclude the possibility that the linkers in our constructs render the S domains to function differently from WT STIM1 and therefore the CRAC channel may have an alternative Orai1-STIM1 stoichiometry.

The graded activation of CRAC channel by binding of different numbers of STIM1 helps to explain a long standing phenomenon in the field that overexpression of Orai1 inhibited endogenous SOCE in HEK293 cells (Figure 3E) [14, 25, 26] and also I_{CRAC} in RBL and Jurkat cells [26, 30]. Our results would predict such an inhibitory effect as the availability of endogenous STIM1 for each Orai1 subunit is reduced upon overexpression of Orai1. Our data (see Figure 3 and Figure 5) indicate that the reduction in the number of available STIM1 for Orai1 should render a nonlinear, much greater decrease in the I_{CRAC} amplitudes.

The graded activation has been reported for other tetrameric channels like the potassium channel [31], the AMPA receptor [32, 33] and the cyclic nucleotide gated (CNG) channel [34]. In contrast to the fact that at least two ligand-bound subunits are required to significantly open the AMPA receptor and the CNG channel, as determined by single channel recording [32, 34], we find that the CRAC channel is partially activated at the macroscopic whole-cell level when only one Orai1 subunit can interact with STIM1. It is unknown which factor – the opening probability, conductance or both of them – is changed during this graded activation process due to the undetectable single channel conductance. Nevertheless, such graded activation would enable the CRAC channel to generate a wide range of I_{CRAC} corresponding to different numbers of STIM1 molecules available, as compared to an "all-or-none" activation mode (the channel opens only when all four subunits are interacting with STIM1). For example, when the ER Ca^{2+} store is partially depleted, which may be the case for most physiological stimulations, only a small amount of STIM1 dissociate with Ca^{2+} and become free to interact with Orai1; the graded activation mechanism we revealed here can ensure the opening of CRAC channels and hence refilling of Ca^{2+} store without concerted binding of all four Orai1 subunits to STIM1. The generation of multiple levels of I_{CRAC} might also contribute to variable $[Ca^{2+}]_i$ levels and oscillation patterns required for differential gene expressions in immune cells [35, 36].

Materials and Methods

Cell culture and transfection

HEK293 cells (ATCC) were cultured in Dulbecco's modified Eagle's medium (DMEM) with 10% heat-inactivated fetal bovine serum, 50 U/ml penicillin and 50 mg/ml streptomycin. Cells were transfected with 1.6 μg DNA using Lipofectamine 2000 (Invitrogen) reagent following the manufacturer's instructions. When the plasmids could generate constitutive I_{CRAC}, 10 μM $LaCl_3$ was added to the culture medium after transfection to avoid the toxicity of spontaneous Ca^{2+} influx. For coexpression experiments, SS-mKO or SS-eGFP was cotransfected with Orai1-derived constructs containing single Orai1 at a mass ratio of 1:1, that containing two-tandem Orai1 at a ratio of 1:2 and that containing four-tandem Orai1 at a ratio of 1:5. Stim1-mOrange and four-tandem mut/WT Orai1 constructs were cotransfected at a ratio of 1:5. Expression of both constructs in each cell was confirmed by the emission fluorescence of eGFP and that of mKO or mOrange. For each set of experiments, the GFP fluorescence of Orai1-derived constructs was measured to confirm that the differences in current amplitudes were not due to differences in expression levels of Orai1 channels (Supplementary information, Figure S4).

Plasmids construction

For the construction of SS-eGFP, the S domain (AAs 336-485 of STIM1) was amplified by PCR using the primers: 5′-GAG CTC GAG GGG GTA CCA AGC CAC CAT GGG TGG ATC CGG CGA ATC TCA CAG CTC ATG G-3′ and 5′-CCG GAT CCC GAA

TTC CAC CTC CGC TAC CTC CAG AGC CGC CCA CAA TCT CCT CAT CCA TC-3′. The fragment was then digested with *Xho*I (5′) and *Eco*RI (3′) and inserted into a pEGFP-N1 (Clontech) vector. Then, the other S fragment was PCR amplified using another forward primer, 5′-GAG CTC GAG GGG TGG ATC CGG TGG GTC CGG CGG ATC CGG CGA ATC TCA CAG CTC ATG G-3′ and the same reverse primer as the first S fragment. This fragment was then inserted downstream of the former-constructed S using *Sal*I (5′) and *BamH*I (3′). A linker sequence of 24 residues was thus generated between the tandem S domains. The mKO-tagged SS was produced by substituting the eGFP sequence with the mKO sequence in the pEGFP-N1 vector.

Construction of Orai1, 2×Orai1 and 4×Orai1 tagged with eGFP or mKO was described previously [17], where an 18-residue linker sequence (MLHPGLSPGLLPLHPASI) was inserted immediately upstream of the N-terminus of each Orai1 sequence. Construction of mOrange-tagged STIM1 was described elsewhere [25].

For the constructions of eGFP-tagged Orai1-S, Orai1-SS, 2×Orai1-SS and 4×Orai1-SS, *Nhe*I (5′) and *Sal*I (3′) flanked Orai1, 2×Orai1 and 4×Orai1 were cut out from the plasmids containing Orai1-eGFP, 2×Orai1-eGFP and 4×Orai1-eGFP. These DNA fragments were ligated into the S-pEGFP-N1 or SS-pEGFP-N1 digested by *Nhe*I (5′) and *Xho*I (3′).

All point mutations were generated on single S or single Orai1 sequence using the standard site-directed mutation protocol and confirmed by sequencing. These mutants were then used to produce constructs containing proper arrangements and numbers of mutant subunits (See Supplementary information, Data S1 for the constructions of other plasmids used in this study).

Western blotting

48 h after transfection, HEK293 cells were washed with PBS and lysed in SDS loading buffer. For Orai1-SS-eGFP in Figure 1B, samples were denatured at 100 °C for 3 min. For 2×Orai1-SS-eGFP and 4×Orai1-SS-eGFP in Figure 3A, samples were loaded without denaturation at 100 °C. Blots were probed with anti-GFP (Santa Cruz Biotechnology, Santa Cruz, CA) antibody according to the standard procedures.

Confocal microscopy

Transfected HEK293 cells were imaged under a confocal laser scanning microscope FV500 (Olympus Optical Co., Tokyo, Japan) in Ca^{2+}-free Ringer's solution containing 155 mM NaCl, 4.5 mM KCl, 2 mM $MgCl_2$, 1mM EGTA, 10 mM D-glucose and 5 mM HEPES (pH 7.4). All experiments were performed at room temperature.

Electrophysiology

Patch clamp experiments were performed at room temperature using standard whole-cell recording configuration as previously described [25]. Cells were plated on poly-L-lysine-coated coverslips 12-24 h before experiments. The extracellular solution contained 140 mM cesium glutamate, 6 mM $CaCl_2$, 2 mM $MgCl_2$, 10 mM tetraethylammonium chloride and 10 mM Hepes (pH 7.4, adjusted with CsOH). For recording of constitutive I_{CRAC}, the pipette was filled with solution containing 140 mM cesium glutamate, 8 mM $MgCl_2$, 10 mM BAPTA, 3.5 mM $CaCl_2$ and 10 mM Hepes (pH 7.2, adjusted with CsOH). The free $[Ca^{2+}]$ of this solution was calculated to be 145 nM using MaxChelator. The pipette solution was added with 10 μM $Ins(1,4,5)P_3$ in some experiments (Figure 4E and Figure 5B) to deplete the Ca^{2+} stores. Before patch clamp recording, the GFP epifluorescence of each cell was excited by a xenon light source at 488 nm and measured at 510 ± 5 nm with a photodiode. After establishment of whole-cell configuration, voltage stimuli consisting of a 10-ms step to −100 mV followed by a 50-ms voltage ramp from −100 to +100 mV were delivered from the holding potential of 0 mV every 2 s. Currents were digitized at a rate of 20 kHz and filtered offline at 2 kHz. All current traces were leak-subtracted. I-V currents were collected by delivering voltage ramps after seal formation and before break-in, and that with current magnitude at +50 mV equal to the sustained outward current after break-in was assigned as leak current. Capacitive currents were determined and corrected before each voltage ramp. The current amplitude at −80 mV of individual ramp was extracted to monitor the development of I_{CRAC} and current amplitudes at −100 mV were used for statistical analysis. Data were analyzed by IGOR Pro 5.01 (Wavemetrics). Averaged results were presented as the mean values ± s.e.m. with the numbers of experiments indicated.

Single cell $[Ca^{2+}]_i$ measurement

HEK293 cells were pre-incubated with 4 μM fura-2/AM (Invitrogen) at 37 °C for 20 min in DMEM. The standard extracellular Ringer's solution contained 145 mM NaCl, 4.5 mM KCl, 2 mM $CaCl_2$, 1 mM $MgCl_2$, 10 mM D-glucose and 5 mM Hepes (pH 7.4, adjusted with NaOH). The $CaCl_2$ was replaced by 1 mM EGTA and 2 mM $MgCl_2$ in Ca^{2+}-free solution. Fluorescence of fura-2 was excited by a dual wavelength excitation (340/380 nm) photometry system on an inverted microscope (IX71, Olympus, Tokyo, Japan) with a polychromatic xenon light source (TILL photonics, Gräfeling, Germany). The emission from a single cell was collected at 510 ± 5 nm with a photodiode controlled by the TILL photometry system and X-Chart extension of Pulse software (HEKA, Lambrecht, Germany). $[Ca^{2+}]_i$ was calculated using fluorescence ratio R (340/380) according to equation $[Ca^{2+}]_i = K_{eff}(R - R_{min})/(R_{max} - R)$ as previously described [25].

Conflict of interest

The authors declare no competing financial interests. Requests for materials should be addressed to TX (xutao@ibp.ac.cn).

Acknowledgments

We thank Professor Roger Y Tsien (University of California at San Diego, La Jolla) for providing the mOrange; Drs Bertil Hille, Erwin Neher, Michael Cahalan and Joy Fleming for careful reading and critical comments on the manuscript; Li Zheng and Junbing Wu for advice on western blotting; Drs Xiaolan Xu, Yong Yu and Lijun Chen for discussion during the project. This work was supported by grants from the National Science Foundation of China (30870564, 30630020), the Major State Basic Research Program of China (2006CB911001, 2010CB833701) and the CAS Project (YZ200838).

References

1 Lewis RS. Calcium signaling mechanisms in T lymphocytes.

Annu Rev Immunol 2001; **19**:497-521.
2 Parekh AB, Putney JW Jr. Store-operated calcium channels. *Physiol Rev* 2005; **85**:757-810.
3 Liou J, Kim ML, Heo WD, *et al*. STIM is a Ca2+ sensor essential for Ca2+-store-depletion-triggered Ca2+ influx. *Curr Biol* 2005; **15**:1235-1241.
4 Roos J, DiGregorio PJ, Yeromin AV, *et al*. STIM1, an essential and conserved component of store-operated Ca2+ channel function. *J Cell Biol* 2005; **169**:435-445.
5 Feske S, Gwack Y, Prakriya M, *et al*. A mutation in Orai1 causes immune deficiency by abrogating CRAC channel function. *Nature* 2006; **441**:179-185.
6 Zhang SL, Yeromin AV, Zhang XH, *et al*. Genome-wide RNAi screen of Ca(2+) influx identifies genes that regulate Ca(2+) release-activated Ca(2+) channel activity. *Proc Natl Acad Sci USA* 2006; **103**:9357-9362.
7 Vig M, Peinelt C, Beck A, *et al*. CRACM1 is a plasma membrane protein essential for store-operated Ca2+ entry. *Science* 2006; **312**:1220-1223.
8 Zhang SL, Yu Y, Roos J, *et al*. STIM1 is a Ca2+ sensor that activates CRAC channels and migrates from the Ca2+ store to the plasma membrane. *Nature* 2005; **437**:902-905.
9 Prakriya M, Feske S, Gwack Y, Srikanth S, Rao A, Hogan PG. Orai1 is an essential pore subunit of the CRAC channel. *Nature* 2006; **443**:230-233.
10 Vig M, Beck A, Billingsley JM, *et al*. CRACM1 multimers form the ion-selective pore of the CRAC channel. *Curr Biol* 2006; **16**:2073-2079.
11 Yeromin AV, Zhang SL, Jiang W, Yu Y, Safrina O, Cahalan MD. Molecular identification of the CRAC channel by altered ion selectivity in a mutant of Orai. *Nature* 2006; **443**:226-229.
12 Xu P, Lu J, Li Z, Yu X, Chen L, Xu T. Aggregation of STIM1 underneath the plasma membrane induces clustering of Orai1. *Biochem Biophys Res Commun* 2006; **350**:969-976.
13 Luik RM, Wu MM, Buchanan J, Lewis RS. The elementary unit of store-operated Ca2+ entry: local activation of CRAC channels by STIM1 at ER-plasma membrane junctions. *J Cell Biol* 2006; **174**:815-825.
14 Mercer JC, Dehaven WI, Smyth JT, *et al*. Large store-operated calcium selective currents due to co-expression of Orai1 or Orai2 with the intracellular calcium sensor, Stim1. *J Biol Chem* 2006; **281**:24979-24990.
15 Park CY, Hoover PJ, Mullins FM, *et al*. STIM1 clusters and activates CRAC channels via direct binding of a cytosolic domain to Orai1. *Cell* 2009; **136**:876-890.
16 Zhou Y, Meraner P, Kwon HT, *et al*. STIM1 gates the store-operated calcium channel ORAI1 *in vitro*. *Nat Struct Mol Biol* 2010; **17**:112-116.
17 Ji W, Xu P, Li Z, *et al*. Functional stoichiometry of the unitary calcium-release-activated calcium channel. *Proc Natl Acad Sci USA* 2008; **105**:13668-13673.
18 Mignen O, Thompson JL, Shuttleworth TJ. Orai1 subunit stoichiometry of the mammalian CRAC channel pore. *J Physiol* 2008; **586**:419-425.
19 Penna A, Demuro A, Yeromin AV, *et al*. The CRAC channel consists of a tetramer formed by Stim-induced dimerization of Orai dimers. *Nature* 2008; **456**:116-120.
20 Maruyama Y, Ogura T, Mio K, *et al*. Tetrameric Orai1 is a teardrop-shaped molecule with a long, tapered cytoplasmic domain. *J Biol Chem* 2009; **284**:13676-13685.
21 Luik RM, Wang B, Prakriya M, Wu MM, Lewis RS. Oligomerization of STIM1 couples ER calcium depletion to CRAC channel activation. *Nature* 2008; **454**:538-542.
22 Hogan PG, Lewis RS, Rao A. Molecular basis of calcium signaling in lymphocytes: STIM and ORAI. *Annu Rev Immunol* 2010; **28**:491-533.
23 Yuan JP, Zeng W, Dorwart MR, Choi YJ, Worley PF, Muallem S. SOAR and the polybasic STIM1 domains gate and regulate Orai channels. *Nat Cell Biol* 2009; **11**:337-343.
24 Mori MX, Erickson MG, Yue DT. Functional stoichiometry and local enrichment of calmodulin interacting with Ca2+ channels. *Science* 2004; **304**:432-435.
25 Li Z, Lu J, Xu P, Xie X, Chen L, Xu T. Mapping the interacting domains of STIM1 and Orai1 in Ca2+ release-activated Ca2+ channel activation. *J Biol Chem*, 2007; **282**:29448-29456.
26 Soboloff J, Spassova MA, Tang XD, Hewavitharana T, Xu W, Gill DL. Orai1 and STIM reconstitute store-operated calcium channel function. *J Biol Chem* 2006; **281**:20661-20665.
27 Muik M, Frischauf I, Derler I, *et al*. Dynamic coupling of the putative coiled-coil domain of ORAI1 with STIM1 mediates ORAI1 channel activation. *J Biol Chem* 2008; **283**:8014-8022.
28 Zhou Y, Meraner P, Kwon HT, *et al*. STIM1 gates the store-operated calcium channel ORAI1 *in vitro*. *Nat Struct Mol Biol* 2010; **17**:112-116.
29 Muik M, Fahrner M, Derler I, *et al*. A Cytosolic homomerization and a modulatory domain within STIM1 C terminus determine coupling to ORAI1 channels. *J Biol Chem* 2009; **284**:8421-8426.
30 Peinelt C, Vig M, Koomoa DL, *et al*. Amplification of CRAC current by STIM1 and CRACM1 (Orai1). *Nat Cell Biol* 2006; **8**:771-773.
31 Zheng J, Sigworth FJ. Intermediate conductances during deactivation of heteromultimeric Shaker potassium channels. *J Gen Physiol* 1998; **112**:457-474.
32 Rosenmund C, Stern-Bach Y, Stevens CF. The tetrameric structure of a glutamate receptor channel. *Science* 1998; **280**:1596-1599.
33 Sobolevsky AI, Rosconi MP, Gouaux E. X-ray structure, symmetry and mechanism of an AMPA-subtype glutamate receptor. *Nature* 2009; **462**:745-756.
34 Ruiz ML, Karpen JW. Single cyclic nucleotide-gated channels locked in different ligand-bound states. *Nature* 1997; **389**:389-392.
35 Dolmetsch RE, Lewis RS, Goodnow CC, Healy Ji. Differential activation of transcription factors induced by Ca2+ response amplitude and duration. *Nature* 1997; **386**:855-858.
36 Dolmetsch RE, Xu K, Lewis RS. Calcium oscillations increase the efficiency and specificity of gene expression. *Nature* 1998. **392**:933-936.
37 Chen Y, Deng Y, Zhang J, Yang L, Xie X, Xu T. GDI-1 preferably interacts with Rab10 in insulin-stimulated GLUT4 translocation. *Biochem J* 2009; **422**:229-235.

(**Supplementary information** is linked to the online version of the paper on the *Cell Research* website.)